



PCCP

Quinonoid vs aromatic structures of heteroconjugated polymers from oligomer calculations

Journal:	<i>Physical Chemistry Chemical Physics</i>
Manuscript ID	CP-ART-02-2020-000606.R1
Article Type:	Paper
Date Submitted by the Author:	15-Apr-2020
Complete List of Authors:	Grover, Girishma ; Georgetown University, Department of Chemistry Peters, Garvin; Johns Hopkins University, Chemistry Tovar, J. D.; Johns Hopkins University, Department of Chemistry Kertesz, Miklos; Georgetown University, Department of Chemistry

SCHOLARONE™
Manuscripts

Quinonoid vs aromatic structures of heteroconjugated polymers from oligomer calculations

Girishma Grover^[1], Garvin Peters^[2], John D. Tovar^{[2, 3]*}, and Miklos Kertesz^{*[1]}

[1] Chemistry Department and Institute of Soft Matter, Georgetown University, 37th and O Streets, NW, Washington, DC, 20057, United States.

[2] Department of Chemistry, Johns Hopkins University, 3400 North Charles Street, Baltimore, Maryland 21218, United States

[3] Department of Materials Science and Engineering, Johns Hopkins University, 3400 North Charles Street, Baltimore, Maryland 21218, United States.

*Corresponding author email: kertesz@georgetown.edu, tovar@jhu.edu

Abstract

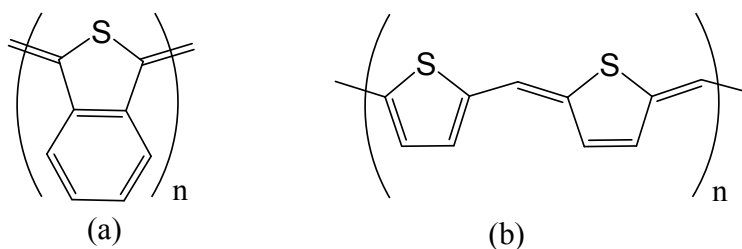
Conjugated polymers with quinonoid ground states can display low optical band gaps. The design of novel conjugated polymers with quinonoid ground states offers insights into the relative stabilities of aromatic vs. quinonoid structures. In this work, we present parameters such as the Quinonoid(Q)/Aromatic(A) energy difference, the band gap, and the C-C distances between the repeat units. This study reveals eight new polymers which exist in quinonoid ground state among twenty-nine polymers of varying structural composition that were subject to analysis. We expect that copolymerizing such quinonoid ground state monomers with aromatic ground state monomers will modulate the bandgap of the resulting polymers.

Introduction

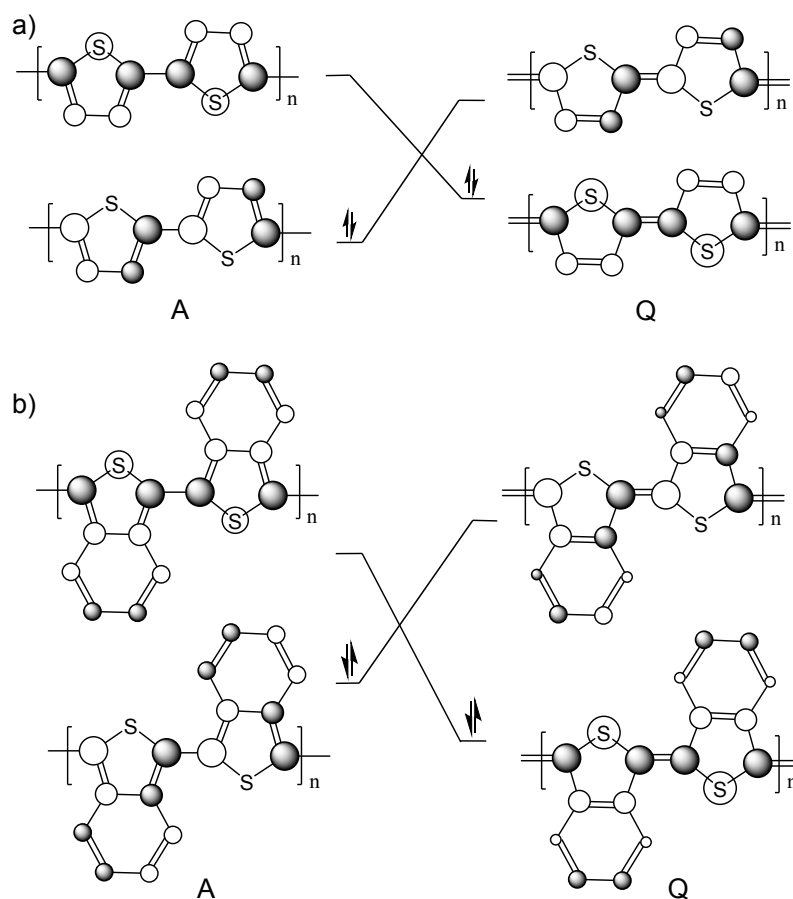
Conjugated polymers constitute a class of materials that have been employed in a wide range of practical applications such as light emitting diodes, field effect transistors, fuel cell electrodes, organic solar cells and chemo sensors because they exhibit high conductivity, good optical properties high hole mobility, synthetic flexibility, and porosity.^[1,2,3,4,5,6]

A small subclass of these polymers has quinonoid linkages connecting the conjugated subunits. The first such polymer, poly(isothianaphthene), PITN, was synthesized by Wudl et al.^[7] and is illustrated in Scheme 1a. The remarkably low bandgap of PITN is related to the level crossing of the highest occupied molecular orbital, HOMO, and lowest unoccupied molecular orbital, LUMO, levels^[8,12] as illustrated in Scheme 2. Another feature of a quinonoid conjugated polymer is that the C-C bond connecting the repeat units is relatively short, an indication of the quinonoid ground state. Quinonoid linkages occur also in methine linked conjugated polymers^[10]

as shown in Scheme 1b. Recent work on mixed aromatic – quinonoid units in conjugated polymers indicates the potentials of this structural motif.^[9]



Scheme 1 (a) Quinonoid structure of the repeat unit of polyisothianaphthene^[7]. (b) Mixed aromatic and quinonoid units in a polymer, with an aromatic and a quinonoid form of thiophene in the repeat unit which contains two rings per structural unit.^[10, 11]



Scheme 2 Level crossing of HOMO and LUMO levels during a geometry change from aromatic (left side) to quinonoid (right side). a) polythiophene (PT), and b) PITN. The A form is more stable for PT, but the Q form is more stable for PITN.^[12]

In this study, we explore the computational design of new members of this unusual subclass of conjugated polymers. These structures may find use as components in co-polymers where the preference for a quinonoid ground state in one unit and an aromatic one in the other

may generate unusual structures with low optical bandgaps. A rare example of this mixed aromatic/quinonoid ground state has been identified in a thiophene derivative illustrated in Scheme 1b ^[10].

Our selection of targets for computational modeling was motivated to include units that are synthetically available or reasonably tractable. The list of targets is shown in scheme 3. Polythiophene (PT) itself prefers the aromatic form over the quinonoid form, however, when the fused benzene ring is attached to thiophene in ITN, the preference changes to quinonoid form, the driving force is the stabilization of the HOMO as illustrated in Scheme 2 along with the accompanying localization of aromaticity in the fused benzene ring.^[12,13] We used heterocyclic analogues of the ITN polymer, such as IBF or II as our primary targets (Scheme 3a) along with an ITN derivative with chloro substituents (ITN-Cl) and ITN polymerized through the fused benzene rings (ITN-6-6). We then moved to analogues of ITN, IBF and II by replacing benzene fusion with pyrazine (Scheme 3b).

The next series, scheme 3c, includes heterocyclic fusion of thiophene or pyrrole with pyrroledione (TPD and PPDO, respectively) or benzoquinone (BTD) to study the effect of these functional groups on the relative stability of the quinonoid vs. the aromatic form.^[14,15] The electron accepting capability of PPDO makes it an attractive model for organic thin film transistors (OTFTs) and organic photovoltaics (OPVs), understanding the effect of fusing electron withdrawing units on the stability of either the quinonoid or the aromatic form will be useful to design such systems in future. ^[16]

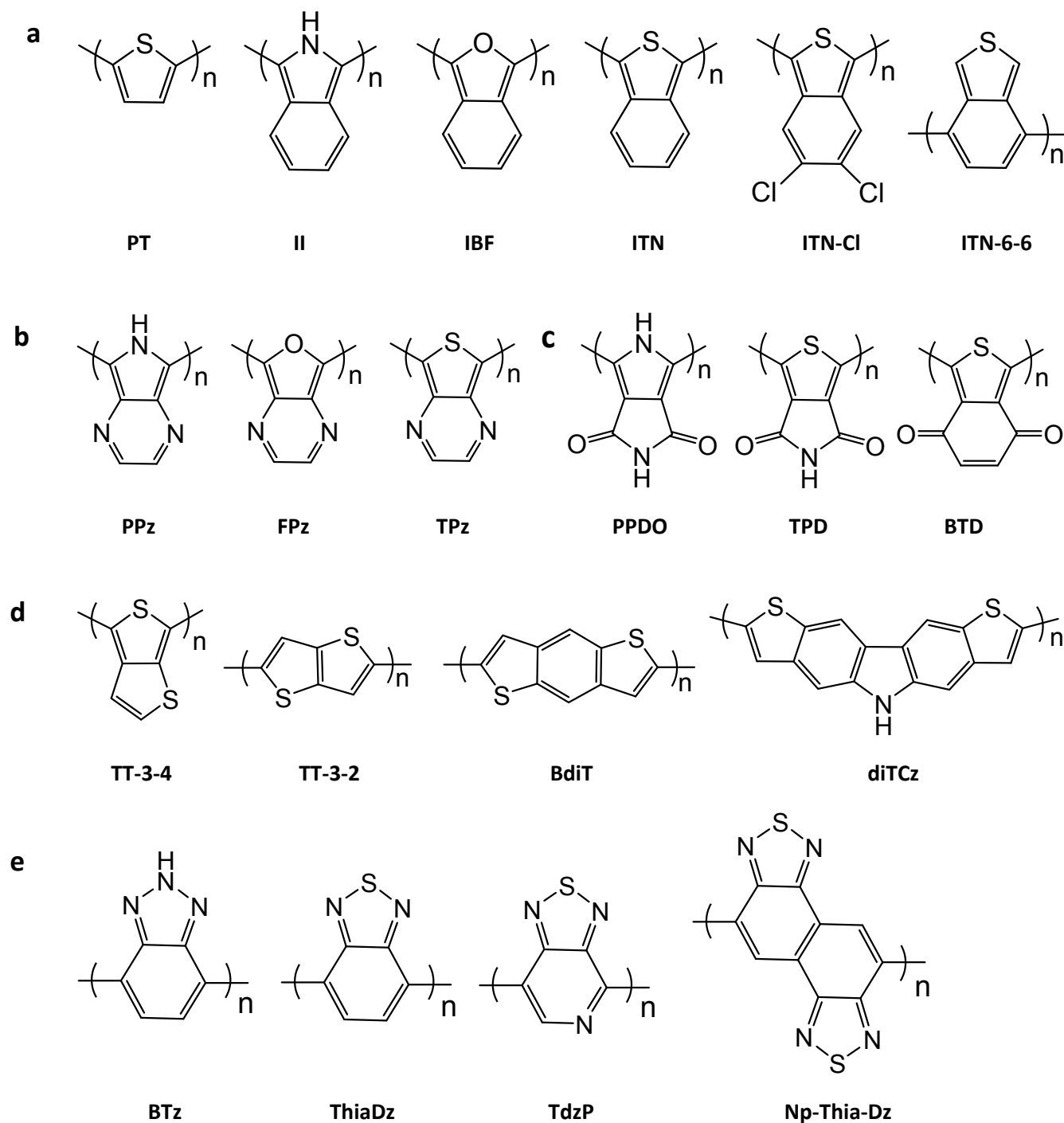
In the next series, we start with fused thiophene rings (TT-3-4) where only one thiophene ring engages in the polymeric backbone and its isomeric variation, TT-3-2, where the entire monomer is engaged in the polymer backbone. We also investigated analogues involving fused benzene rings and pyrrole rings (BdiT and diTCz) shown in Scheme 3d.

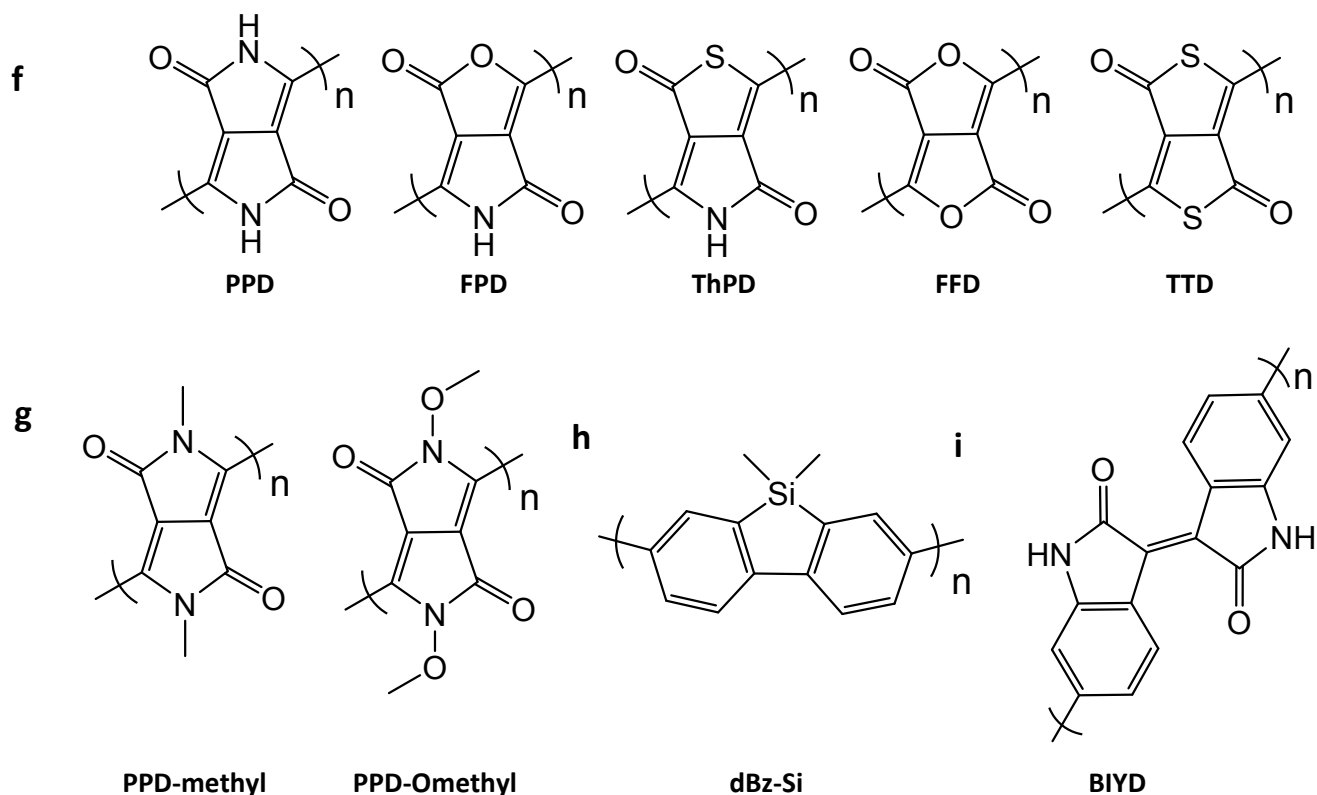
Next, we moved to systems such as benzo[c][1,2,5]thiadiazole and its derivatives along with benzotriazole (Scheme 3e) where the polymer is linked via six-membered rings. The thiadiazole based copolymers have been synthesized and studied extensively in the field of organic solar cells and light emitting diodes(LEDs) due to their low band gap and good charge transport ability.^[17,18] Similarly, the electron-deficient benzotriazole system (BTz) has been studied extensively in donor–acceptor copolymers in photovoltaics, the availability of sites which can be easily functionalized to obtain desirable properties makes this system an attractive model for organic semiconductors. ^[19]

In the next series, we introduced analogues inspired by the 2,5-dihydropyrrolo[3,4-c]pyrrole-1,4-dione core (PPD), Scheme 3f. The PPD monomer has been incorporated into various polymer systems exhibiting excellent photophysical properties. ^[20] Scheme 3f also displays a series of PPD derivatives where one of the pyrrol-2-one ring or both the fused rings are substituted with furan-2-one (FPD and FFD, respectively) or thiophen-2-one (ThPD or TTD, respectively) rings. After observing that the quinonoid form of PPD is more stable than the

aromatic form, we included further derivatives of PPD (Scheme 3g) with functionalizing nitrogens with methyl and methoxy groups (PPD-methyl and PPD-Omethyl).

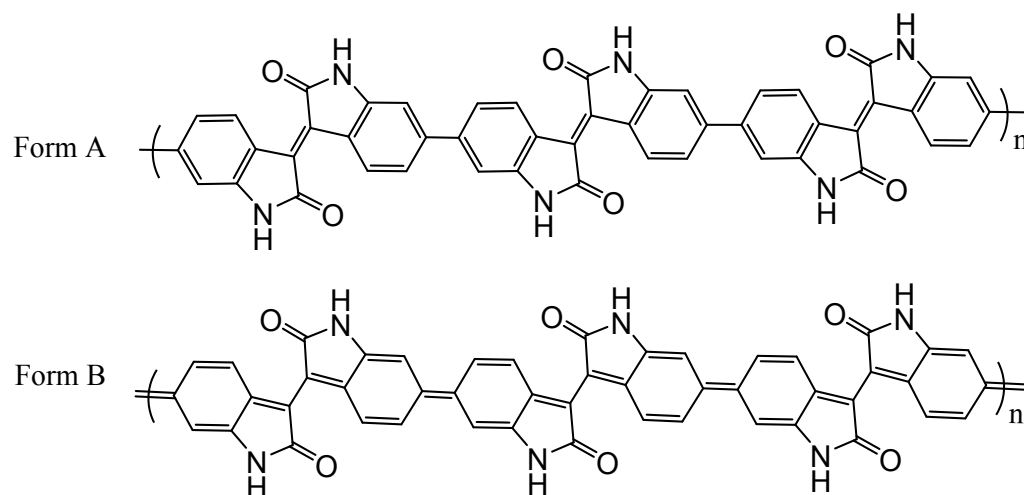
Our next target is poly(dimethyldibenzosilole), which is a derivative of polyfluorene, Scheme 3h, a wide band gap light emitting polymer.^[21] The coplanarity of the repeat unit and its ease of functionalization at the silicon atom make it an attractive candidate for our study.





Scheme 3 Nine groups of repeat units targeting the design of quinonoid ground state polymers.

Scheme 3i represents another PPD analogue, BIYD polymer (poly(E)-[3,3'-biindolynylidene]-2,2'-dione) based on the indigo dye monomer. The BIYD monomer itself contains two indole-2-one units within the structural repeat unit. This polymer has a unique distribution of alternating single and double bonds between adjacent heterocyclic rings similar to the structure shown in Scheme 1b because the chemical repeat unit has an odd number of π -electrons. The Form A of BIYD polymer has a double bond between two adjacent indole-2-one units and a single bond between two adjacent phenyl units, while the Form B has the double bond between two adjacent phenyl units and the single bond between two adjacent indole-2-one units (Scheme 4). Both the Forms A and B have alternating aromatic and quinonoid characters. Calculations on aromatic and quinonoid structures of all the polymers in Scheme 3 provides insight into the relative stability of the aromatic vs. quinonoid forms of these unique systems.



Scheme 4 Forms A and B of the BIYD polymer with the alternating aromatic and quinonoid character analogous to the polymer in Scheme 1b.

Methods

Geometry optimizations were performed using density functional theory (DFT) calculations on a different number of heteroconjugated oligomers with the PBE0/6-31G(d) method with the Gaussian 16 package^[22,23,24,25]. The oligomers were terminated with $-H$ to represent the aromatic structure and with the $=CH_2$ group to represent the quinonoid structure.^[26] Our approach was to determine whether the polymer chain consisting of heteroconjugated monomers exists in an aromatic form or a quinonoid form. We determined the stability and properties of the two forms by a variety of parameters such as the Quinonoid(Q)/Aromatic(A) energy difference, the band gap, and the C-C distance (r) between adjacent central heteroconjugated rings in each of the oligomers.

We studied different oligomer sizes with n repeat units (with n values up to 5) for both quinonoid and aromatic structures. For these systems, the energy of a single monomeric unit of a polymer in the aromatic structure, $E_A(n)$, as well as the quinonoid structure, $E_Q(n)$, was obtained from the difference in the energy of two largest consecutive n -mers in that structure.

$$E_A(n) = E_A^{(n)} - E_A^{(n-1)} \quad (1)$$

$$E_Q(n) = E_Q^{(n)} - E_Q^{(n-1)} \quad (2)$$

where $E_A^{(n)}$ is the energy of the n -mer in the aromatic structure and $E_Q^{(n)}$ is the energy of the n -mer in the quinonoid structure. The largest n values for each molecule are given in Table S2. For example, in case of ITN, $E_A(5)$ was obtained from the difference of the optimized energy of the ITN pentamer and the ITN tetramer in the aromatic structure, the largest available oligomers.

The Q/A energy difference, $\Delta E(n)$, was further calculated from the difference of $E_A(n)$ and $E_Q(n)$ in each case by equation (3) and plotted in Fig. 1. Negative values indicate quinonoid preference, positive indicate aromatic preference.

$$\Delta E(n) = E_Q(n) - E_A(n) \quad (3)$$

We also calculated HOMO-LUMO gap for all n-mers in each of the systems for both the aromatic and the quinonoid structure.

$$Eg_A(n) = E_A^{(HOMO)}(n) - E_A^{(LUMO)}(n) \quad (4)$$

$$Eg_Q(n) = E_Q^{(HOMO)}(n) - E_Q^{(LUMO)}(n) \quad (5)$$

where $E_A^{(HOMO)}(n)$ and $E_Q^{(HOMO)}(n)$ is the energy of HOMO orbital for n-mer in the aromatic structure and the quinonoid structure, and $E_A^{(LUMO)}(n)$ and $E_Q^{(LUMO)}(n)$ is the energy of LUMO orbital for n-mer in the aromatic structure and the quinonoid structure, respectively.

We used a linear extrapolation method to obtain the extrapolated band gap (Eg_A and Eg_Q) for different polymeric systems with both their aromatic and quinonoid structures, by plotting the band gaps of n-mers ($Eg_A(n)/Eg_Q(n)$) as a function of $1/n$.^[27] Alternatives to linear extrapolation^[28,29] are discussed as well as an example of this calculation are shown in Table S1 and Fig. S2 in the SI.

Results and Discussion

Quinonoid vs. aromatic energy difference

Fig. 1 shows the Q/A energy difference, ΔE , between the quinonoid and the aromatic form in all the systems under study. Among all the systems, we calculated FFD, FPD, FPz, IBF, ITN, ITN-Cl, PPD, ThPD, and TPz to have lower energy quinonoid forms (i.e. negative $\Delta E(n)$ values). These quinonoid ground state systems will be discussed in detail based on their $\Delta E(n)$ values.

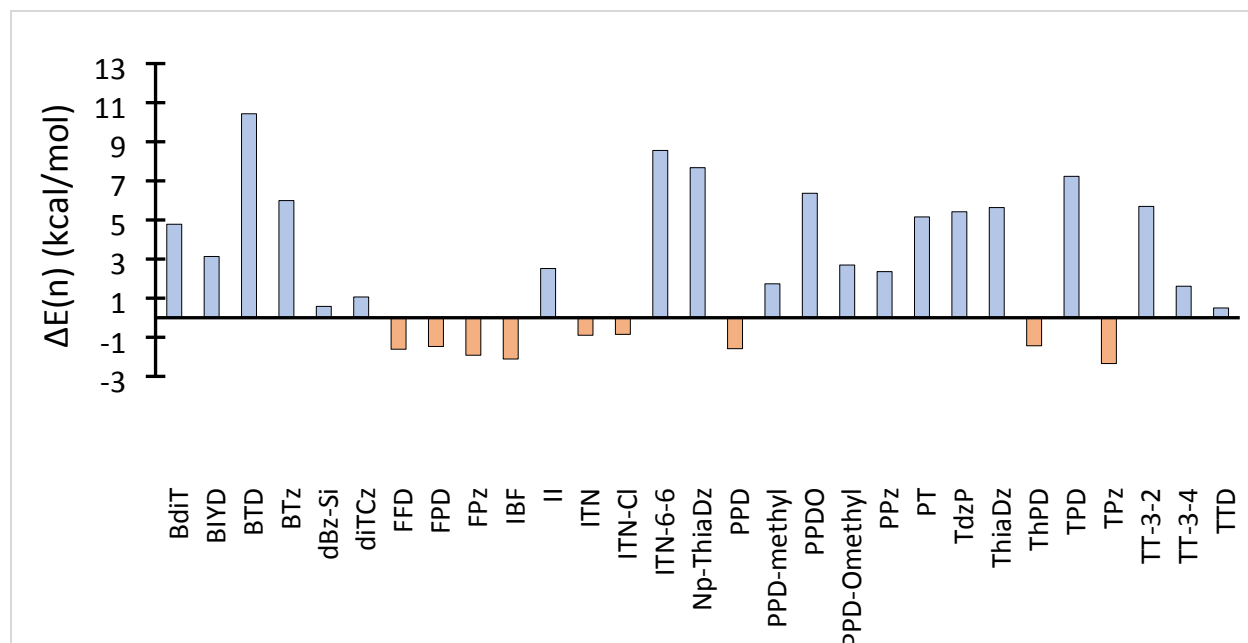


Fig. 1 The Q/A energy difference, $\Delta E(n)$, (kcal/mol) between aromatic and quinonoid structures of heteroconjugated polymers calculated by PBE0/6-31G(d) based on equations (1), (2), and (3). The relevant oligomer sizes, given by the n values, are listed in Table S2. For BIYD, the positive difference refers to a more stable form A vs. form B, see Scheme 4. The repeat units are illustrated in Scheme 3.

The conjugated polymer based on isothianaphthene (ITN) has been studied extensively due to its very small band gap and its ground-state preference of the quinonoid form over the aromatic form.^[12,30,31,32] From our calculations on oligomers, we found that the quinonoid form of ITN is 0.9 kcal/mol more stable than the aromatic form. These calculations were extended to ITN analogue, TPz, in which carbons are replaced by nitrogen at positions 1,4. It appears that the electron withdrawing nitrogen pulls the electron density into the aromatic 6-membered ring making the Q form more stable. Further, the van der Waals distance between S---N is 3.35 Å. The short S---N non-bonded distances in the Q form of TPz obtained are between 2.903-2.907 Å and in the A form are between 2.957-2.960 Å. These short S...N non-bonded distances promote planarity in the oligomers in both forms (Fig. 2a, b).^[33,34] In accordance with this observation, the quinonoid form of TPz is favored by 3.0 kcal/mol compared to the aromatic form, becoming a better candidate for a quinonoid polymeric systems than PITN.

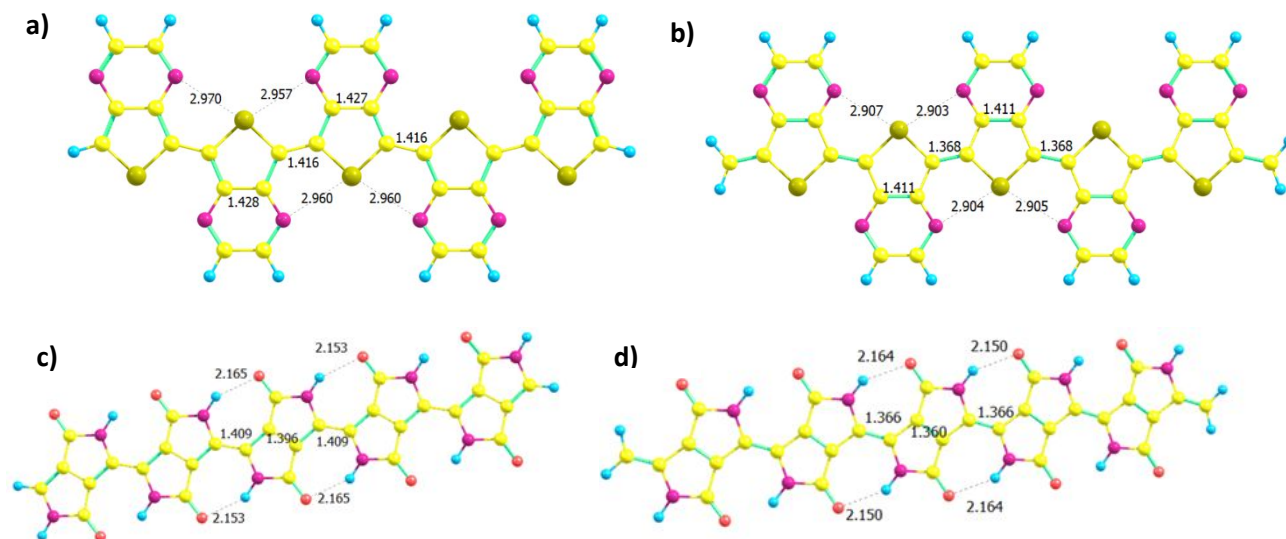


Fig. 2 The optimized geometry of the pentamer of TPz in the a) aromatic structure terminated by -H and the b) quinonoid structure terminated by =CH₂ and pentamer PPD of in the c) aromatic structure terminated by -H and the d) quinonoid structure terminated by =CH₂.

The oligomer calculations performed on heterocyclic analogues of ITN (IBF and II) were compared (Scheme 3a). We observed that sulfur and oxygen analogues, ITN and IBF, prefer the quinonoid form whereas the nitrogen-based analog, II, prefers the aromatic form. The oligomers of IBF exist in a planar conformation while those of ITN exist in a non-planar conformation, for both their quinonoid and aromatic forms. This can be accounted for by the greater stability of the quinonoid form of IBF when compared to that of ITN. The analogues of ITN, IBF and II with fused pyrazine instead of benzene rings (TPz, FPz and PPz, respectively) show a similar trend where the TPz and FPz polymers prefer the quinonoid form while the nitrogen-based analogue, PPz, prefers the aromatic form in the ground state (Scheme 3b). These systems, where the polymer linkage runs through the six- π -electron five membered rings of the monomer, display the quinonoid ground state to some degree because the fused six- π -electron six-membered rings maintain stronger local aromaticities at the expense of the polymer backbone. ITN, IBF, TPz, FPz, ITN-Cl all fall in this category. Exceptions are II and PPz, both pyrrole derivatives.

Turning to polymers with linkage via the six- π -electron six membered rings and with fused six- π -electron five-membered rings we observed that they all prefer an overall aromatic structure. For the thiadiazole derivatives fused with benzene (ThiaDz) or with pyridine (TdzP), we observed that the aromatic form is favored over the quinonoid form in both cases by ~ 6 kcal/mol (Scheme 3e).

In the case of PPD, both the aromatic and the quinonoid forms adopt planar structures due to strong N-H...O hydrogen bonding interactions between adjacent monomeric units (Fig. 2c,d). The planarity and comparatively short hydrogen bonding distances in the Q form likely contribute to its stability over the A form, although the difference is small (only 1.6 kcal/mol). The effects of minor N-substitutions are interesting (Scheme 3g). N-methyl (PPD-methyl) and N-

methoxy (PPD-Omethyl) substitutions on PPD cause a reversal of the A vs. Q stability due to the non-planarity induced by the steric effects (Fig. 3). This leads to a stabilization of the aromatic structure by 1.73 and 2.70 kcal/mol, respectively, and an increase in their bandgap values.

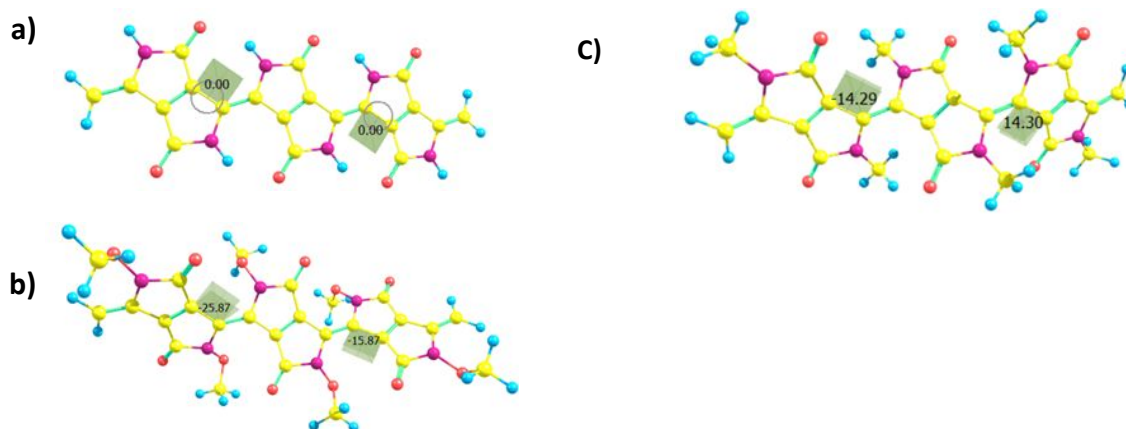


Fig. 3 The optimized geometry of the trimer of a) PPD, b) PPD-Omethyl, and c) PPD-methyl in their quinonoid structures terminated by =CH₂ groups.

The PPD analogues such as FPD and ThPD (Scheme 3f), where one pyrrol-2-one ring from PPD is substituted with furan-2-one or thiophene-2-one, have stable quinonoidal ground states as compared to the aromatic forms by 1.47 and 1.44 kcal/mol, respectively. This stability is enhanced by the presence of hydrogen bonding within one pyrrol-2-one ring, ranging from 1.7 to 2.1 Å. For PPD analogues where both the pyrrol-2-one rings are replaced with either furan-2-one (FFD) or thiophen-2-one (TTD), hydrogen bonding is absent. The FFD polymer is still planar and prefers quinonoidal ground state by 1.61 kcal/mol, while, the TTD polymer loses its planarity due to steric repulsion between the sulfur and the carbonyl units and resulting in a more stable aromatic ground state. Although the TTD system favors the aromatic form, it stands out among other such aromatic ground state systems displaying a very small ΔE value. With increasing n -mer, its $\Delta E(n)$ value decreases ($\Delta E(3) = 0.72$ kcal/mol, $\Delta E(4) = 0.53$ kcal/mol and $\Delta E(5) = 0.50$ kcal/mol). TTD may be considered a borderline case.

Bandgap

Bandgaps of heteroconjugated polymers for aromatic as well as quinonoid forms obtained from a linear extrapolation process are shown in Fig. 4 and S1. We observed that the band gaps correlate with stability: the gap is larger for whichever form is more stable, in line with general expectations. The only exceptions to these correlations between Q/A energy difference and band gaps are ITN and ITN-Cl. Negative extrapolated band gap values appeared for eleven polymers for their quinonoid forms (Fig. S1). The unphysical negative gaps indicate that a level crossing discussed in connection with Scheme 2 appeared when starting from a quinonoid form leading to a more stable aromatic form.^[30] The polymers having stable quinonoid ground states have small quinonoid band gaps ranging between 1 to 2 eV with the smallest being 1.08 eV for

ThPD (Fig. 4). These quinonoid ground state systems have the potential in designing co-polymers with low band gaps.

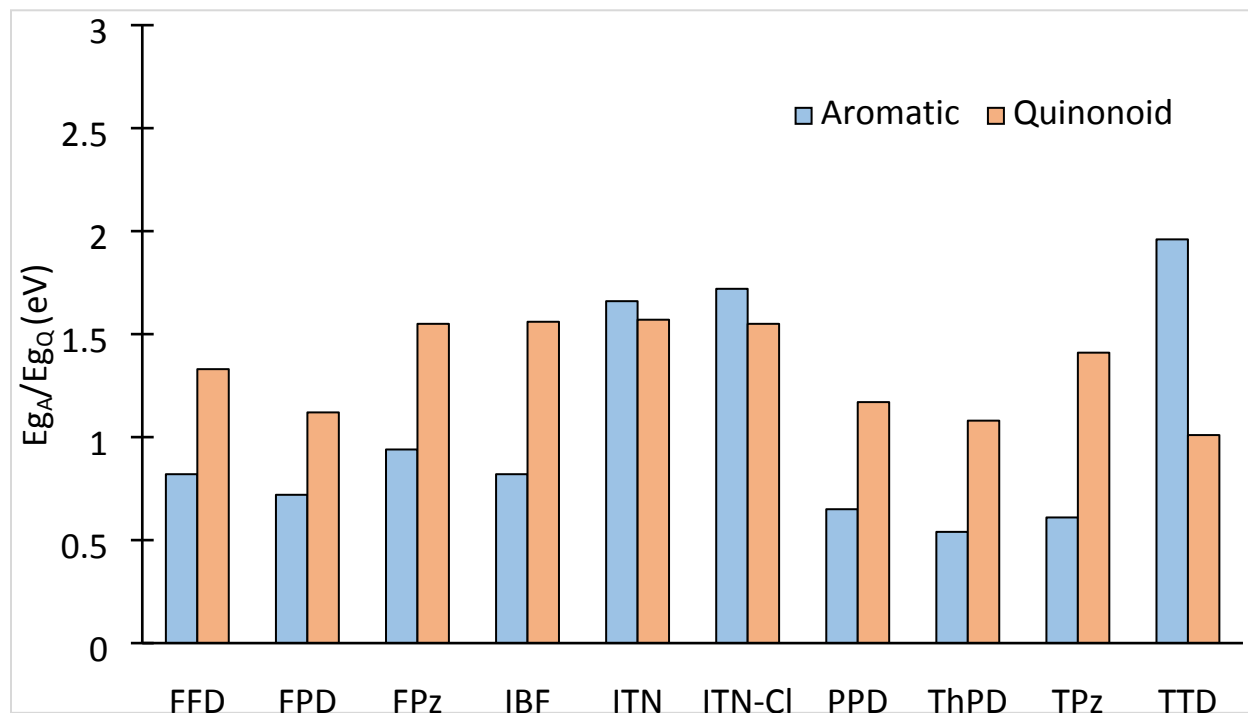


Fig. 4 The band gap values (eV) of heteroconjugated polymers for their optimized aromatic structures, E_{gA} , (blue) and for their quinonoid structures, E_{gQ} , (orange) obtained by linear extrapolation from calculation of different n -mers optimized by the DFT method PBE0/6-31G(d). The respective n values are given in Table S2. All system listed here have a quinonoid ground state except for TTD, a borderline case, see Fig. 1. The repeat units are illustrated in Scheme 3.

Bond distances

Bond distances along the conjugation path are essential to characterize the structures of conjugated polymers and their aromaticity.^[13-15^{Error! Bookmark not defined.},35] The bond distances between the adjacent central heterocyclic rings (r_{C-C}), for different number of n -mers, for the aromatic structures were plotted in Fig. S3-S5. We observed that in most cases, on increasing n in the calculations, r_{C-C} decreases. This shows that on increasing n , the system becomes more stable and conjugated. In some cases, like diTCz, BIYD, TPD and dBz-Si there is no significant change in r_{C-C} as a function of n . We have an exception in BTd, where r_{C-C} increases for the dimer and then decreases for trimer. In PPDO the r_{C-C} increases constantly as oligomer size is increased. The reason for this exception in PPDO appears to be due to steric repulsions between adjacent oxygen atoms.

On the other hand, r_{C-C} increases upon increasing n in the quinonoid structures as can be seen in Fig. S4. In all polymers under study, this gradual increase in r_{C-C} from tetramer to pentamer is small for ITN, IBF, ThPD, TPz and PPD which are systems where the quinonoid form is energetically more stable (Fig. 6). The calculations up to pentamer for the quinonoid structure

of these systems indicate that convergence of the r_{C-C} distance is nearly complete beyond the tetramer. However, for systems with the aromatic form being more stable, the changes of r_{C-C} are significant in their respective quinonoid structures and indicate convergence approaching the r_{C-C} value in the aromatic structure,^[30] the only exception being PPD-Omethyl (Fig. S4).

Data on systems where the polymer linkage is established via 6-membered ring to 6-membered ring CC bonds, between two adjacent central repeat units in the polymer are collected in Fig. S5a. We did not observe stable quinonoid forms in any of these polymers. The preference for the aromatic structure in this group is the clearest for ITN-6-6 where steric repulsions contribute to the elongation of this bond destabilizing the quinonoid structure as compared to ITN. BIYD, which contains both 5-5 and 6-6 interring bonds, steric repulsion would destabilize Form B, illustrated in Scheme 4. In the rest of the group, it appears that the key factor is the relative stability of the Clar sextet in the benzene unit, leading to the larger stability of Form A. Similarly, the aromatic (A) form is more stable for ITN-6-6, see Scheme S1.

We observed a trend with direct CC linkages between the repeat units via 6-membered ring to 6-membered ring where the r_{C-C} value in the quinonoid structures of the pentamers has either already or almost approached the r_{C-C} value of the pentamers in the aromatic structure in agreement with trends seen earlier (Fig. S5a) ^[30]. This trend, as noted by Kurti and Surjan^[30], is an indication that the quinonoid structure forced with the =CH₂ termination at the end of the oligomer cannot flip the whole structure, and the middle of the oligomer is assuming the most stable form, which is the aromatic in this case, as the oligomer size is increased.

dBz-Si is an interesting borderline case similar to TDD with a small positive $\Delta E(n)$. The r_{C-C} distance in its Q form already approached the r_{C-C} distance of the A form (~ 1.47 - 1.48 Å) in the trimer (Fig. S5a), and there is no further increase in the r_{C-C} distance from the tetramer to the pentamer within the Q series. All the oligomers in both the A and the Q forms deviate from planarity with the pentamer of the A form having interring torsions of 37° , while in the Q form this value is only slightly toward the middle of the pentamer (Fig. 5). This could be due to the quinonoid like character of the end rings due to the attachment of =CH₂ group, while the rings in the middle starts to develop aromatic like character. The linear extrapolated band gap of the A form is around 3.51 eV and for the Q form its around -0.55 eV (Fig. S1), which is consistent with the trend we observed where the stable form has the higher band gap. The electron density of pentamer is delocalized over HOMO and LUMO in the A form and localized at the terminal in HOMO and LUMO of the Q form (Fig. 5). Further, the HOMO is more stabilized in the A form (-5.393 eV) than in the Q form (-3.562 eV) and LUMO is more stabilized in the Q form (-3.463 eV) than in the A form (-1.519 eV). These observations show a preference for aromatic structure which is also confirmed by A/Q energy difference (Fig. 1) where the A form is the more stable ground state of the two.

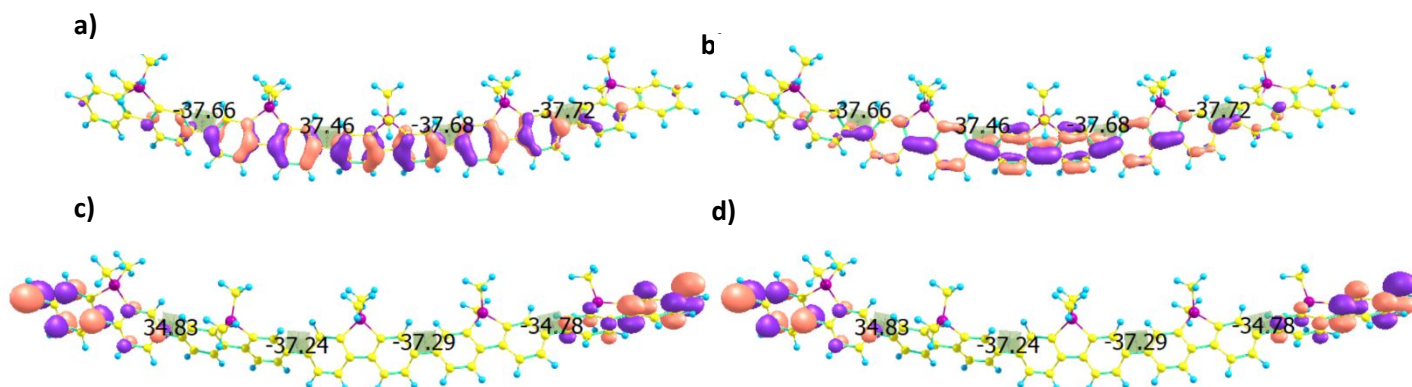


Fig. 5 The optimized geometry of the pentamer of dBz-Si showing the dihedral angles between two rings and delocalization of the a) HOMO, and b) LUMO orbitals in the aromatic structure terminated by -H; and the c) HOMO, and d) LUMO orbitals in the quinonoid structure terminated by =CH₂.

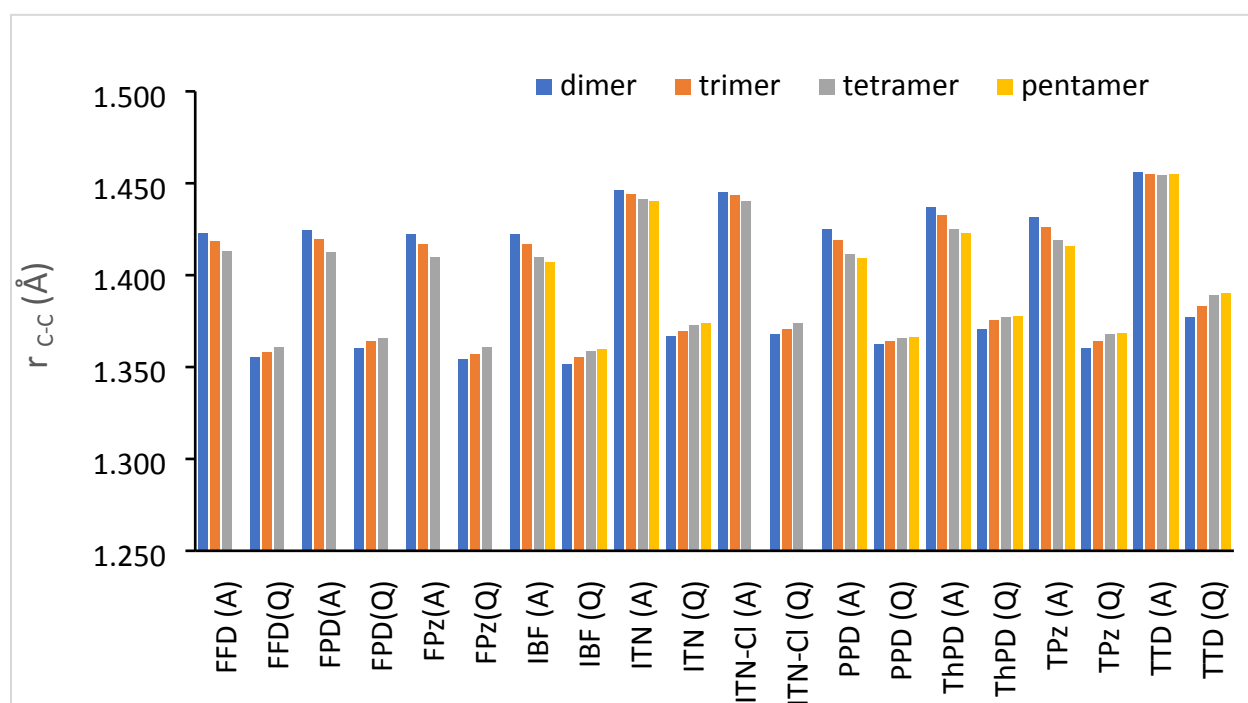


Fig. 6 Plot of CC distances, r_{C-C} , between two adjacent central repeat units for all polymer with a quinonoid ground state discussed in this paper plus a borderline case (TTD). Based on optimized geometries of oligomers as shown by PBE0/6-31G(d). The respective n values are given in Table S2. The repeat units are illustrated in Scheme 3.

Fig. 7 represents the optimized geometry of the pentamer of ThiaDz in its aromatic and quinonoid structures. The large twisting between adjacent monomers ($\sim 29.1^\circ$) in the aromatic structure increases the N-H distance (2.32 Å), thus, minimizing the steric hindrance between the two adjacent rings with $r_{C-C} = 1.47$ Å as compared small twisting ($\sim 8.5^\circ$) in the quinonoid structure which caused a steric hindrance between the adjacent N-H (2.08 Å) with $r_{C-C} = 1.42$ Å. This

repulsion between the adjacent N-H due to small r_{C-C} value makes the quinonoid structure energetically less stable (Fig. 1).

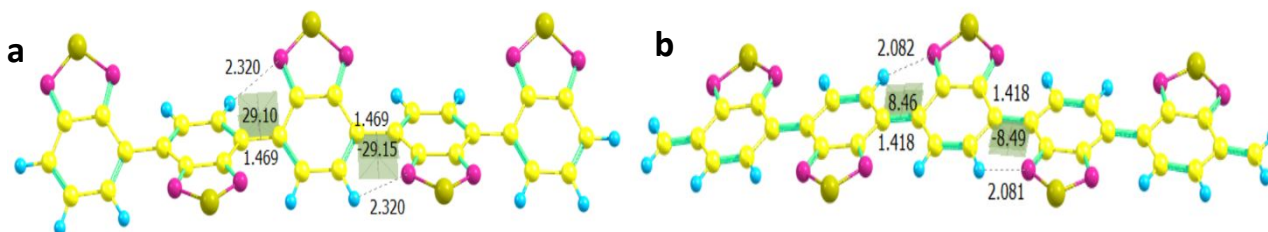


Fig. 7 The optimized geometry of pentamer of ThiaDz in the a) aromatic structure terminated by H and the b) quinonoid structure terminated by $=CH_2$ with r_{C-C} and adjacent N-H distance.

Moving on to the oligomers of heterocyclic polymers linked with adjacent monomers via 5-membered ring to 5-membered ring, we observed stable quinonoid forms for some of the systems under study. These adjacent central r_{C-C} values in Fig. S5b approach typical quinone-like values when the quinonoid form is more stable and again, aromatic-like values when the aromatic form is more stable. For the systems like IBF, PPD, ThPD, TPz, and ITN, this change is small and indicates again the relative stability of the quinonoid forms in good agreement with the Q/A energy differences discussed in connection with the data in Fig. 1. TTD, a borderline case is an exception to this trend.

Conclusions

Using a computational approach, we explored the ground-state aromatic and quinonoid structures of twenty-nine heteroaromatic polymers based on monomers that are synthetically accessible. We identified eight new polymers with quinonoid ground states that are energetically more stable than their counterparts with aromatic isomeric structures. Some of these polymers also possess relatively small band gaps. The possibility of these polymers to exist in the quinonoid ground state was further confirmed using other parameters such as the band gap and inter-ring r_{C-C} bond lengths between adjacent central heteroconjugated rings in each of the oligomers.

The presence of inter-unit hydrogen bonding often contributes to the reduction of the inter-unit CC bond length tipping the subtle balance in favor of the quinonoid structure as seen in case of PPD, FPD and ThPD. On the other hand steric crowding near the inter-unit CC bond typically destabilizes the quinonoid form in PPD-methyl, PPD-Omethyl, TTD, BTM, PPDO and ThiaDz. The non-bonded interactions between sulfur and nitrogen shortens the S...N non-bonded distances contributing to planarity of oligomers and favoring the quinonoid form of TPz. The polymers linked via 5-membered rings in their backbones tend to prefer a quinonoid ground state relative to those that are linked via 6-membered rings. With the intent to engineer the band gap of conjugated polymers, we plan to copolymerize these Q ground state and A ground state monomers with the expectation that some of these combinations might result in very low band gaps.

Acknowledgements. This material is based upon work supported by the U.S. Department of Energy, Office of Science, Office of Basic Energy Sciences under Award Number DE-SC-0019017.

References

- ¹ M. Atesa, T. Karazehira and A. S. Sarac, *Curr. Phys. Chem.*, 2012, **2**, 224-240.
- ² Z. Bao, A. Dodabalapur and A. Lovinger, *J. Appl. Phys. Lett.*, 1996, **69**, 4108-4110.
- ³ G. Li, V. Shrotriya, Y. Yao, and Y. Yang, *J. Appl. Phys.*, 2005, **98**, 043704.
- ⁴ L. Chen, D. W. Mcbranch, H. L. Wang, R. Helgeson, F. Wudl and D. G. Whitten, *Proc. Natl. Acad. Sci. USA*, 1999, **96**, 12287-12292.
- ⁵ J. H. Burroughes, D. D. C. Bradley, A. R. Brown, R. N. Marks, K. Mackay, R. H. Friend, P. L. Burns and A. B. Holmes, *Nature*, 1990, **347**, 539-541.
- ⁶ A. J. Appleby and E. B. Yeager, *Energy*, 1986, **11**, 137-152.
- ⁷ F. Wudl, M. Kobayashi and A. J. Heeger, *J. Org. Chem.*, 1984, **49**, 3382-3384.
- ⁸ J. L. Bredas, F. Wudl and A. J. Heeger, *J. Chem. Phys.*, 1986, **85**, 4673
- ⁹ C. L. Anderson, N. Dai, S. Teat, B. He, S. Wang and Y. Liu, *Angew. Chem. Internat. Ed.*, 2019, **58**, 17978-17985.
- ¹⁰ S. A. Jenekhe, *Nature*, 1986, **322**, 345-347.
- ¹¹ M. Kertesz and Y. S. Lee, *J. Phys. Chem.*, 1987, **91**, 2690-2692.
- ¹² Y. S. Lee and M. Kertesz, *Int. J. Quantum Chem.*, 1987, **21**, 163-170.
- ¹³ M. Kertesz, C. H. Choi and S. J. Yang, *Chem. Rev.* 2005, **105**, 3448-3481.
- ¹⁴ N. Bérubé, J., Gaudreau, and M. Côté, *Macromolecules*, 2013, **46**, 6873-6880.
- ¹⁵ Y. Hayashi, and S. Kawauchi, *Polym. Chem.*, 2019, **10**, 5584-5593.
- ¹⁶ C. Guo, B. Sun and Y. Li, *Polym. Chem.*, 2014, **5**, 5247-5254.
- ¹⁷ M. Saito, I. Osaka, Y. Suzuki, K. Takimiya, T. Okabe, S. Ikeda, and T. Asano, *Scientific reports*, 2015, **5**, 14202.
- ¹⁸ P. Camurlu and N. Guven, *J. Appl. Polym. Sci.*, 2015, **132**, 42206.
- ¹⁹ S. Yum, T. K. An, X. Wang, W. Lee, M. A. Uddin, Y. J. Kim, T. L. Xu, S. Nguyen, S. Hwang, C. E. Park and H. Y. Woo, *Chem. Mater.*, 2014, **26**, 2147-2154.
- ²⁰ Y. Zhu, A. R. Rabindranath, T. Beyerlein and B. Tieke, *Macromolecules*, 2007, **40**, 6981-6989.
- ²¹ K. L. Chan, M. J. McKiernan, C. R. Towns and A. B. Holmes, *J. Am. Chem. Soc.*, 2005, **127**, 7662-7663.
- ²² C. Adamo and V. Barone, *J. Chem. Phys.*, 1999, **110**, 6158-6170.
- ²³ P. C. Hariharan and J. A. Pople, *Theor. Chem. Acc.*, 1973, **28**, 213-222.
- ²⁴ W. J. Hehre, R. Ditchfield and J. A. Pople, *J. Chem. Phys.*, 1972, **56**, 2257-2261.
- ²⁵ M. J. Frisch, G. W. Trucks, H. B. Schlegel, G. E. Scuseria, M. A. Robb, J. R. Cheeseman, G. Scalmani, V. Barone, G. A. Petersson, H. Nakatsuji, X. Li, M. Caricato, A. V. Marenich, J. Bloino, B.

G. Janesko, R. Gomperts, B. Mennucci, H. P. Hratchian, J. V. Ortiz, A. F. Izmaylov, J. L. Sonnenberg, D. Williams-Young, F. Ding, F. Lipparini, F. Egidi, J. Goings, B. Peng, A. Petrone, T. Henderson, D. Ranasinghe, V. G. Zakrzewski, J. Gao, N. Rega, G. Zheng, W. Liang, M. Hada, M. Ehara, K. Toyota, R. Fukuda, J. Hasegawa, M. Ishida, T. Nakajima, Y. Honda, O. Kitao, H. Nakai, T. Vreven, K. Throssell, J. A. Montgomery, Jr., J. E. Peralta, F. Ogliaro, M. J. Bearpark, J. J. Heyd, E. N. Brothers, K. N. Kudin, V. N. Staroverov, T. A. Keith, R. Kobayashi, J. Normand, K. Raghavachari, A. P. Rendell, J. C. Burant, S. S. Iyengar, J. Tomasi, M. Cossi, J. M. Millam, M. Klene, C. Adamo, R. Cammi, J. W. Ochterski, R. L. Martin, K. Morokuma, O. Farkas, J. B. Foresman and D. J. Fox, Gaussian 16, Gaussian, Inc., Wallingford CT, 2016.

²⁶ A. Karpfen and M. Kertesz, *J. Phys. Chem.*, 1991, **95**, 7680-7681.

²⁷ S. Yang, P. Orlishevski and M. Kertesz, *Synth. Met.*, 2004, **141**, 171–177.

²⁸ J. Torras, J. Casanovas and C. Alemán, *J. Phys. Chem. A*, 2012, **116**, 7571-7583.

²⁹ R. E. Larsen, *J. Phys. Chem. C*, 2016, **120**, 9650-9660.

³⁰ J. Kurti, and P. Surjan, *J. Chem. Phys.*, 1990, **92**, 3247-3248.

³¹ H. Meng and F. Wudl, *Macromolecules*, 2001, **346**, 1810-1816.

³² S. A. Chen and C. C. Lee, *Polymer*, 1996, **37**, 519-522.

³³ N. E. Jackson, B. M. Savoie, K. L. Kohlstedt, M. Olvera de la Cruz, G. C. Schatz, L. X. Chen, and M. A. Ratner, *J. Am. Chem. Soc.* 2013, **135**, 10475-83.

³⁴ G. Raos, A. Famulari, S. V. Meille, M. C. Gallazzi, and G. Allegra, *J. Phys. Chem. A*, 2004, **108**, 691-698.

³⁵ T. M. Krygowski, H. Szatyłowicz, O. A. Stasyuk, J. Dominikowska, and M. Palusiak, *Chem. Rev.* 2014, **114**, 6383-6422.